

## Enhanced Transverse Diffusion in Active Biomembranes

R. Granek and S. Pierrat

*Department of Materials and Interfaces, Weizmann Institute of Science, Rehovot 76100, Israel*

(Received 6 January 1999)

We study the transverse diffusion of a tagged membrane point in membranes that include active sites, such as ion pumps. At very short times we find a subdiffusive behavior  $\langle r^2 \rangle \sim t^{2/3}$  as for passive membranes. At long times we find a few regimes which show a strongly enhanced diffusion,  $\langle r^2 \rangle \sim t^\alpha$  with  $1 < \alpha < 2$ . One of the regimes shows a purely ballistic motion  $\alpha = 2$ .

PACS numbers: 87.16.Uv, 87.15.Vv, 87.16.Dg

Lipid and surfactant membrane bilayers deserved much attention in the past two decades [1,2]. While the interest in these membranes has been very wide, ranging from determining fundamental concepts of fluctuating surfaces to very practical applications, one key motivation has been their possible role as simple models for biomembranes. Most of the studies focused on the stiffness of a membrane bilayer to bending and stretching, the statistics of its thermal undulations, and the different phases in which it appears in, and out of, equilibrium.

Biomembranes include, however, among other additional constituents, carrier proteins that act as active transport sites [3], for example, the ATPase controlling the  $\text{Na}^+$ - $\text{K}^+$  pump. These sites use chemical energy (ATP), or sometimes the free energy stored in a chemical potential gradient of another type of ions, in order to “pump” a solute ion or molecule against its chemical potential gradient. When an ion is transferred from one side of the membrane to the other through an active channel, the membrane is using force to do work on the ion. By “Newton’s third law,” the ion exerts the same force on the membrane in the opposite direction. Since ion transfer is a stochastic process, these ion transfers induce a force noise, in addition to the thermal noise which results from collisions of the solvent molecules with the membrane. In addition to their stochastic function, ion channels are also able to diffuse around within the two dimensional membrane surface, which leads to another source of force fluctuations.

The effect of this active noise on the mean square amplitude of membrane undulations has been recently studied by Prost and Bruinsma and their co-workers [4,5]. They found that the active noise strongly enhances undulation fluctuations at long distances. This suggests that active membranes behave quite differently from passive membranes even in terms of physical quantities which are not directly related to their activity. Even though this is certainly not the main reason for the presence of active carrier proteins in plasma membrane, nature may have been able to take advantage of this “side effect” behavior.

The mean square amplitude (equal time correlation function) presents only part of the characteristics of the active noise driven undulations. A more complete information lies in dynamic quantities. In this paper we focus on the

transverse mean square displacement (MSD) of a tagged membrane “monomer.” For passive membranes we have previously found that thermal bending modes lead to an anomalous *subdiffusion*, with a MSD increasing as  $t^{2/3}$  [6,7]. (Regular diffusion is described by a MSD increasing linearly with time.) Below, we show that active noise enhances the diffusion greatly. Even though, in general, the MSD cannot be described by a single power law, we find a few distinct regimes in time for which the MSD increases as  $\sim t^\alpha$  with  $\alpha > 1$ . Such MSD power laws are termed *enhanced* diffusion. They have been found theoretically in various generic and novel models [8], but are rare for complex fluid systems. Except for its physical importance, the enhanced diffusion may have implications on the biological functionality of the membrane as well.

Consider first the energy cost to slightly bend a piece of membrane according to a given (Monge gauge) displacement field  $h(\vec{\rho})$ , where  $\vec{\rho}$  is a 2D vector on the base (planar) surface. This can be described by the Helfrich free energy [9], evaluated for small deformations  $\nabla h \ll 1$ ,

$$H = \frac{1}{2} \kappa \int d^2\rho [\nabla^2 h(\vec{\rho})]^2 = \frac{1}{2L^2} \sum_{\vec{q}} \kappa q^4 h_{\vec{q}} h_{-\vec{q}}, \quad (1)$$

where  $\kappa$  is the bending modulus,  $h_{\vec{q}} = \int d^2\rho e^{i\vec{q}\cdot\vec{\rho}} h(\vec{\rho})$  is the 2D Fourier transform of  $h(\vec{\rho})$ , and  $L$  is the membrane linear size. The term  $\nabla^2 h(\vec{\rho})$  is the mean curvature written for small deformations. In the main part of the Letter, we assume that the tension vanishes, even though a certain amount of tension usually exists in living cells. However, the tension can be tuned down to zero in a carefully designed experiment, by tuning the osmotic pressure difference between interior and exterior of the cell. We shall briefly comment on the effect of tension before the end.

Following Prost and Bruinsma [4,5], active sites of a surface density  $n_0$  are introduced to the membrane. The local density of active site  $n(\vec{\rho}, t)$  is assumed to *fluctuate* according to a diffusion equation on the membrane surface [10]. Thus, the dynamic structure factor of active sites is decaying according to

$$\langle n_{\vec{q}}(t) n_{-\vec{q}}(0) \rangle = \langle n_{\vec{q}} n_{-\vec{q}} \rangle e^{-D_c q^2 t}, \quad (2)$$

where  $D_c$  is the collective diffusion coefficient. For a trace of the motion of a single site in the membrane, the MSD is taken to follow the common simple diffusion law,

$$\langle [\vec{\rho}_j(t) - \vec{\rho}_j(0)]^2 \rangle = 4D_s t, \quad (3)$$

where  $D_s$  is the self-diffusion coefficient. For simplicity, we shall assume (as in Ref. [4]) that the density of sites is small enough so that they can be regarded as noninteracting; in this case  $\langle n_{\vec{q}} n_{-\vec{q}} \rangle = n_0$  (and  $D_c = D_s$ ). The activity of each site  $j$  is also assumed to *fluctuate* in time (in a given direction, in or out, which will not be allowed to fluctuate for simplicity) and is described by a stationary stochastic variable  $S_j(t)$ , which has a mean  $\langle S_j(t) \rangle = \bar{S}$  and fluctuates in time between 0 (probability  $1 - \bar{S}$ ) and 1 (probability  $\bar{S}$ ). The temporal force exerted on the membrane at a site  $j$  is then  $f_j(t) = \Gamma S_j(t)$  (for a typical channel  $\Gamma \sim k_B T/a$ , where  $a$  is the membrane thickness  $a \sim 20\text{--}50$  Å). Different sites are assumed to operate independently of each other. Adopting the “random telegraph process” model for these gate fluctuations [11], the correlation function for  $S_j(t)$  obeys

$$\langle S_i(t) S_j(t') \rangle = \bar{S}^2 + \delta_{i,j} g_0 e^{-|t-t'|/\tau}, \quad (4)$$

with  $g_0 = \bar{S}(1 - \bar{S})$ .

The Langevin equation of motion for the displacement field  $h(\vec{\rho}, t)$  which corresponds to this model is [4]

$$\frac{\partial h(\vec{\rho}, t)}{\partial t} = - \int d^2 \rho' \Lambda(|\vec{\rho} - \vec{\rho}'|) \kappa \nabla_{\rho'}^4 h(\vec{\rho}', t) + \lambda_p F(\vec{\rho}, t) + \zeta(\vec{\rho}, t). \quad (5)$$

Here,  $\zeta(\vec{\rho}, t)$  is the thermal white noise,  $\Lambda(\rho) = 1/8\pi\eta\rho$  is the Oseen hydrodynamic interaction kernel [12] (with  $\eta$  the solvent viscosity),  $\lambda_p$  is the permeation constant, and  $F(\vec{\rho}, t)$  represents the active noise (force per unit area) and

is given by

$$F(\vec{\rho}, t) = \sum_j \delta(\vec{\rho} - \vec{\rho}_j(t)) f_j(t). \quad (6)$$

We have dropped on the right-hand side of Eq. (5) the term  $\lambda_p \kappa \nabla_{\rho}^4 h(\vec{\rho}, t)$  which is negligible for small wave numbers obeying  $4\eta\lambda_p q \ll 1$ . For typical values of  $\lambda_p$  [5,13],  $\lambda_p \sim 10^{-5}$  cm<sup>2</sup> s/g, this corresponds to wavelengths and times of interest:  $\lambda \gg 200$  Å,  $t \gg 10^{-9}$  s. Fourier transforming ( $\vec{\rho} \rightarrow \vec{q}$ ), Eq. (5) leads to

$$\frac{\partial h_{\vec{q}}(t)}{\partial t} = -\omega_q h_{\vec{q}}(t) + \lambda_p F_{\vec{q}}(t) + \zeta_{\vec{q}}(t), \quad (7)$$

where the relaxation frequency  $\omega_q$  is given by [14]

$$\omega_q = \frac{\kappa q^3}{4\eta}. \quad (8)$$

The correlation function of  $\zeta_{\vec{q}}(t)$  is assumed to be the same as in the passive membrane case [ $F_{\vec{q}}(t) = 0$ ], for which it is deduced from the fluctuation-dissipation theorem to be  $\langle \zeta_{\vec{q}}(t) \zeta_{-\vec{q}}(t') \rangle = 2k_B T \Lambda(q) \delta(t - t')$ . This amounts to assuming that the function of ion pumps does not influence the thermal collisions between the solvent molecules and the membrane.

Note that since  $\langle F(\vec{\rho}, t) \rangle = n_0 \Gamma \bar{S}$  the membrane center of mass drifts at a constant velocity  $V_{\text{dr}} = \lambda_p n_0 \Gamma \bar{S}$  in the transverse direction. If the experiment is done with vesicles of mean radius  $R$  (instead of free membranes as assumed here for simplicity), the membrane cannot drift but a tension  $\sigma$  may be induced,  $\langle F \rangle = 2\sigma/R$ . We shall assume, however, that  $\langle F \rangle$  is carefully balanced by an osmotic pressure difference to give a vanishingly small net tension. Note also that in a spherical geometry our Fourier expansion is admissible only for  $qR \gg 1$ , which means that only the short time evolution (prior to saturation, see below) is accurately described.

We first solve for the nonequal time correlation function in a *stationary (steady) state* to obtain

$$\frac{1}{L^2} \langle h_{\vec{q}}(t) h_{-\vec{q}}(0) \rangle_s = \frac{k_B T}{\kappa q^4} e^{-\omega_q t} + \frac{\lambda_p^2 \Gamma^2 n_0 \bar{S}^2}{\omega_q (\omega_q^2 - \alpha_q^2)} [\omega_q e^{-\alpha_q t} - \alpha_q e^{-\omega_q t}] + \frac{\lambda_p^2 \Gamma^2 n_0 g_0}{\omega_q (\omega_q^2 - \beta_q^2)} [\omega_q e^{-\beta_q t} - \beta_q e^{-\omega_q t}], \quad (9a)$$

where

$$\alpha_q = D_c q^2; \quad \beta_q = \frac{1}{\tau} + D_s q^2. \quad (9b)$$

For  $t = 0$ , Eq. (9a) reduces to the result of Prost and Bruinsma [4].

Using Eq. (9a) we can calculate the transverse MSD of a tagged membrane point [7]  $\langle [\Delta h(t)]^2 \rangle_s \equiv \langle [h(\vec{\rho}, t) - h(\vec{\rho}, 0) - V_{\text{dr}} t]^2 \rangle_s$ . The result may be written in the form  $\langle [\Delta h(t)]^2 \rangle_s = \langle [\Delta h(t)]^2 \rangle_{\text{th}} + \lambda_p^2 \Gamma^2 n_0 [\bar{S}^2 \langle [\Delta h(t)]^2 \rangle_{CD} + g_0 \langle [\Delta h(t)]^2 \rangle_{SS}]$ . (10)

The first term in Eq. (10) is the thermal undulations contribution discussed in Refs. [6,7]. At times short compared to the saturation time  $\sim \eta L^3/\kappa$  it increases as  $(k_B T/\kappa^{1/3} \eta^{2/3}) t^{2/3}$ . The second and third terms are the contribution of active sites: The second term is due to the noise generated by the collective diffusion of active sites, and the third term is due to the noise generated at a given membrane point both from the random operation of a single active center near that point and from its diffusion

out of that region. We now discuss the two active noise terms in turn.

The collective diffusion contribution is given by

$$\langle [\Delta h(t)]^2 \rangle_{CD} = \frac{1}{\pi} \int_{\pi/L}^{\pi/a} dq q \frac{\alpha_q}{\omega_q^2 - \alpha_q^2} \times \left[ \frac{1 - e^{-\alpha_q t}}{\alpha_q} - \frac{1 - e^{-\omega_q t}}{\omega_q} \right]. \quad (11)$$

[Note that this does not have the units of  $[L]^2$ , cf. Eq. (10).] The evolution described by Eq. (11) is complicated but may be simplified to two main regimes:

$$\langle [\Delta h(t)]^2 \rangle_{CD} \simeq \begin{cases} 1.62 D_c (\frac{\eta}{\kappa})^{4/3} t^{5/3} & \text{for } t \ll t_{c1}^* \\ \frac{1}{2\pi D_c} t \ln(\frac{t}{t_{c1}^*}) & \text{for } t \gg t_{c1}^*, \end{cases} \quad (12)$$

where  $t_{c1}^* = \kappa^2/16\eta^2 D_c^3$ . Note that the evolution for  $t \ll t_{c1}^*$  presents a marked *enhanced diffusion*, with an exponent  $5/3$ , which is significantly larger than unity. This shows that the active nonequilibrium noise strongly enhances the motion, in contrast to the thermal, bending energy controlled undulations which lead to a subdiffusive motion [6,7]. The long time regime  $t \gg t_{c1}^*$  is characterized by an almost regular diffusion and will show up only for  $L \gg \kappa/\eta D_c$ .

For the numerical analysis, we write Eq. (11) in the scaling form  $\langle [\Delta h(t)]^2 \rangle_{CD} = C f(\theta_c, t/\tau_b)$  where  $C = (4\eta L^2/\kappa)^2$ ,  $\tau_b = 4\eta L^3/\kappa$  is the bending hydrodynamic relaxation time (and determines the MSD saturation time,  $\tau_s = \tau_b/\pi^3$ ), and  $\theta_c = 4\eta D_c L/\kappa$  is the ratio of  $\tau_b$  to  $\tau_D = L^2/D_c$ , the lateral diffusion time over a distance  $L$ . In Fig. 1 we plot  $f(\theta_c, t/\tau_b)$  against the reduced time  $t/\tau_b$  for  $\theta_c = 100$ , e.g., when  $\kappa = 10k_B T$ ,  $L = 100 \mu\text{m}$ , and  $D_c = 10^{-7} \text{cm}^2/\text{s}$ . This implies  $\tau_s \sim 10^4 t_{c1}^*$ . We can

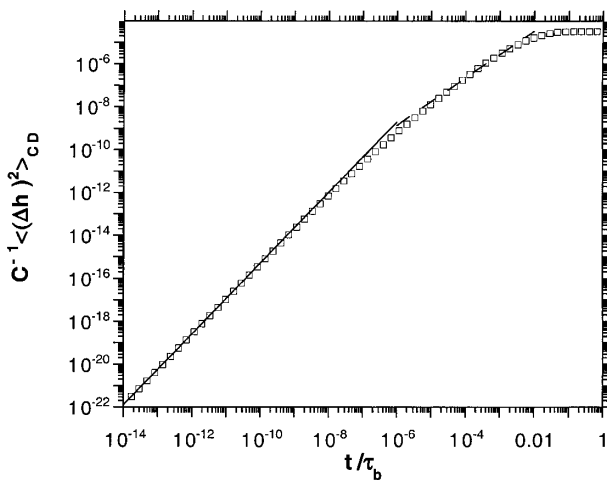


FIG. 1. The contribution of collective site diffusion to the transverse MSD [Eq. (11)]. The MSD (symbols), divided by  $C = (4\eta L^2/\kappa)^2$ , is plotted against  $t/\tau_b$ , where  $\tau_b = 4\eta L^3/\kappa$ , for  $\theta_c = 4\eta D_c L/\kappa = 100$ . The full line is a power-law fit for  $t/\tau_b < 10^{-10}$ :  $y \sim t^\alpha$ ,  $\alpha = 1.649$ . The dashed line is a guide to the eye for the  $t \ln t$  regime in Eq. (12).

clearly note the  $t^{5/3}$  regime at short times, and the  $t \ln t$  regime at long times, before saturation occurs.

Next we deal with the contribution of the single site noise to the MSD. This takes the form

$$\langle [\Delta h(t)]^2 \rangle_{SS} = \frac{1}{\pi} \int_{\pi/L}^{\pi/a} dq q \frac{\beta_q}{\omega_q^2 - \beta_q^2} \times \left[ \frac{1 - e^{-\beta_q t}}{\beta_q} - \frac{1 - e^{-\omega_q t}}{\omega_q} \right]. \quad (13)$$

If  $4\eta D_s/\kappa \ll 1/\sqrt{D_s \tau}$ , which is obeyed in most typical situations (see range of parameter values below), the evolution is

$$\langle [\Delta h(t)]^2 \rangle_{SS} \simeq \begin{cases} 1.62 D_s (\frac{\eta}{\kappa})^{4/3} t^{5/3} & \text{for } t \ll t_{s3}^* \\ \frac{1}{2\pi} (\frac{4\eta}{\kappa \tau})^{2/3} t^2 & \text{for } t_{s3}^* \ll t \ll \tau \\ 1.08 \tau (\frac{\eta}{\kappa})^{2/3} t^{1/3} & \text{for } t \gg \tau, \end{cases} \quad (14)$$

where  $t_{s3}^* = (\eta \tau/\kappa)^2 D_s^3$ . Quite unexpectedly, we have  $\langle [\Delta h(t)]^2 \rangle_{SS} \sim t^2$  in the intermediate regime, which corresponds to a purely *ballistic* motion and is presumably the strongest enhanced diffusion possible for this model.

The numerical evaluation of Eq. (13) is depicted in Fig. 2 for a typical case corresponding to  $\eta D_s/\kappa \ll 1/\sqrt{D_s \tau}$ . The  $t^{5/3}$  increase at short times is followed, at  $t/\tau_b > 10^{-13}$ , by a nearly perfect power law  $t^\alpha$  with  $\alpha \simeq 1.89$ , which is close to the  $\alpha = 2$  obtained in Eq. (14). (The small discrepancy is due only to the too narrow time regime in this case.) For  $t/\tau_b > 10^{-7}$  we clearly show in Fig. 2 the  $t^{1/3}$  regime.

Consider now the overall MSD [Eq. (10)]. The numerical evaluation for one typical case is plotted in Fig. 3. At

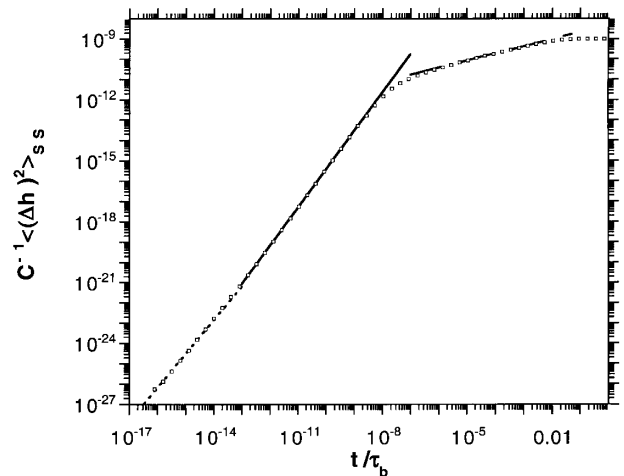


FIG. 2. The contribution of single site noise to the transverse MSD [Eq. (13)]. The MSD (symbols), divided by  $C = (4\eta L^2/\kappa)^2$ , is plotted against  $t/\tau_b$  for  $\theta_s = 4\eta D_s L/\kappa = 10$  and  $\tau_b/\tau = 10^8$ . The short dashed line is a power-law fit for  $t/\tau_b < 10^{-14}$ :  $y \sim t^\alpha$ ,  $\alpha = 1.655$ . The full line is a power-law fit for  $10^{-12} < t/\tau_b < 10^{-9}$ :  $\alpha = 1.886$ . The long dashed line is a power-law fit for  $10^{-4} < t/\tau_b < 10^{-2}$ :  $\alpha = 0.351$ .

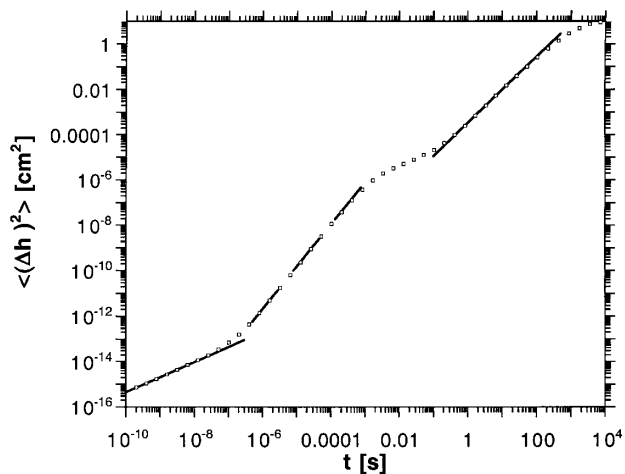


FIG. 3. Transverse MSD (symbols), in  $\text{cm}^2$ , against the time, in seconds, corresponding to the following parameter values:  $\eta = 10^{-2}$  poise,  $\lambda_p = 10^{-5}$   $\text{cm}^2 \text{s/g}$ ,  $\Gamma = 10^{-5}$  dyn,  $n_0 = 4 \times 10^{12}$   $\text{cm}^{-2}$ ,  $\kappa = 10k_B T$ ,  $\bar{S} = 0.1$ ,  $g_0 = \bar{S}(1 - \bar{S}) = 0.09$ ,  $\tau = 10^{-3}$  s,  $D_c = D_s = 10^{-8}$   $\text{cm}^2/\text{s}$ , and  $L = 10^{-2}$  cm. These parameters correspond to  $\theta_c = \theta_s = 10$  and  $\tau_b/\tau = 10^8$ . The lower full line is a power-law fit for  $t < 10^{-8}$  s:  $y \sim t^\alpha$ ,  $\alpha = 0.661$ . The dashed line is a power-law fit for  $10^{-6} < t < 5 \times 10^{-5}$  s:  $\alpha = 1.865$ . The upper full line is a power-law fit for  $1 < t < 10$  s:  $\alpha = 1.461$ .

very early times, which may not be practically reached in experiment, the  $t^{2/3}$  of the thermal undulations always dominates. A crossover to the active noise regime occurs at some time  $t_a^*$  ( $t_a^* \sim 10^{-6}$  s in Fig. 3), which we estimate to be (for typical cases where  $t_{s3}^* \ll t_a^* \ll \tau$ )  $t_a^* \sim \kappa^{1/4} (k_B T)^{3/4} \tau^{1/2} / [\eta (\lambda_p^2 \Gamma^2 n_0 g_0)^{3/4}]$ . Taking [5,13]  $\kappa \sim 10k_B T$ ,  $\lambda_p \sim 10^{-5}$   $\text{cm}^2 \text{s/g}$ ,  $n_0 \sim 4 \times 10^{12}$   $\text{cm}^{-2}$ ,  $g_0 \sim 0.1$  ( $\bar{S} \sim 0.1$ ),  $\eta = 10^{-2}$  poise,  $\tau \sim 10^{-3}$  s [15], and  $\Gamma \sim 10^{-5} - 10^{-6}$  dyn, we find  $t_a^*$  in the range  $t_a^* \sim 10^{-7} - 10^{-5}$  s, a rather short time. Consistently, we have  $\eta D_s / \kappa \ll 1 / \sqrt{D_s \tau}$  (with  $D_s \sim 10^{-7} - 10^{-9}$   $\text{cm}^2/\text{s}$ ) and  $t_{s3}^* \sim 10^{-12} - 10^{-6}$  s, so that in most cases  $t_{s3}^* \ll t_a^* \ll \tau$ , as assumed. The active noise regime is first dominated by the  $\sim t^2$  single site contribution ( $\sim t^{1.87}$  in Fig. 3 due to a too narrow regime). Just as the latter starts to cross over (at  $t \sim \tau$ ,  $\tau = 10^{-3}$  s in Fig. 3) to a  $\sim t^{1/3}$  increase, the collective site contribution, which evolves as  $t^{5/3}$ , becomes dominant. This occurs at times  $t_b^* \sim (g_0 \tau / \bar{S}^2 D_c)^{3/4} (\kappa / \eta)^{1/2}$  ( $t_b^* \sim 0.1$  s in Fig. 3). The  $t^{5/3}$  evolution continues up to times  $t \sim t_{c1}^*$ . For  $D_c$  in the range  $D_c = 10^{-7} - 10^{-9}$   $\text{cm}^2/\text{s}$ , we find  $t_{c1}^*$  in the range  $t_{c1}^* \sim 0.1 - 10^5$  s, which means that it usually is much greater than  $t_b^*$ . In Fig. 3 we find, for  $t > 1$  s, nearly a perfect power law  $\sim t^{1.46}$ , which corresponds to the end of the  $t^{5/3}$  regime as it crosses over to a (narrow)  $t \ln t$  regime and saturation.

Finally, we comment on the effect of tension, which suppresses both the thermally and the actively excited undulations. If the tension  $\sigma$  is so large such that  $\eta \kappa^{1/2} / \sigma^{3/2} < t_a^*$ , a crossover to a tension dominated evolution [7]  $\sim \ln t$  occurs already for  $t < t_a^*$  (thermal undulations

regime), and the active noise regime  $t > t_a^*$  is entirely influenced by tension rather than by bending energy. The leading evolution for  $t > t_a^*$  is then  $\sim t$ , noticeably stronger than  $\ln t$ . (This, however, later crosses over to a  $\sim \ln t$  growth and saturation.) Thus, the enhancement due to active noise is also visible under tension, and can be clearly detected in experiment.

Our analysis shows that, in most typical cases relevant to plasma membranes, the active noise strongly dominates over the thermal noise in a wide range of time, ranging from a microsecond to many seconds. The predicted enhanced diffusion,  $\text{MSD} \sim t^\alpha$ , with  $1 < \alpha < 2$  depending on the time regime, makes a clear fingerprint for the presence of such active noise. The time scale ranging from a fraction of a second to the seconds range makes this evolution amenable to enhanced videomicroscopy studies, whereas the microseconds to milliseconds range can be studied by dynamic light scattering. It is possible that living cells use this enhanced diffusion for their needs, e.g., as an efficient dynamic probe of the environment.

It is a pleasure to thank M. Elbaum, A. Caspi, S. Safran, and J. Klafter for stimulating discussions.

- [1] S.A. Safran, *Statistical Thermodynamics of Surfaces, Interfaces, and Membranes*, Frontiers in Physics Vol. 90 (Addison-Wesley, Reading, MA, 1994).
- [2] *Structure and Dynamics of Membranes*, edited by R. Lipowsky and E. Sackmann (Elsevier, Amsterdam, 1995).
- [3] B. Alberts *et al.*, *Molecular Biology of The Cell* (Garland, New York, 1994), 3rd ed.
- [4] J. Prost and R. Bruinsma, *Europhys. Lett.* **33**, 321 (1996).
- [5] J. Prost *et al.*, *Eur. Phys. J. B* **1**, 465 (1998).
- [6] A.G. Zilman and R. Granek, *Phys. Rev. Lett.* **77**, 4788 (1996).
- [7] R. Granek, *J. Phys. II (France)* **7**, 1761 (1997).
- [8] J. Klafter *et al.*, in *The Physics of Complex Systems*, Proceedings of The International School of Physics "Enrico Fermi," Course CXXXIV, edited by F. Mallamace and H.E. Stanley (IOS press, Amsterdam, 1997).
- [9] W.F. Helfrich, *Z. Naturforsch.* **28C**, 693 (1973).
- [10] P.F.F. Almeida and W.L.C. Vaz, in *Structure and Dynamics of Membranes* (Ref. [2]), Chap. 6.
- [11] C.W. Gardiner, *Handbook of Stochastic Methods* (Springer-Verlag, New York, 1994).
- [12] M. Doi and S.F. Edwards, *The Theory of Polymer Dynamics* (Clarendon, Oxford, 1986), pp. 88–89.
- [13] This value is inferred from permeation measurements on liposomes of size  $R \sim 100$  nm [D. Huster *et al.*, *Biophys. J.* **73**, 855 (1997)]. Typical measured values of permeation "coefficient" (rate)  $P_d$  are  $P_d \sim 100$   $\mu\text{m/s}$ . Using  $P_d = \lambda_p \Delta P$  and  $\Delta P \sim \kappa / R^3$  for the pressure difference between interior and exterior, with  $\kappa \sim 10k_B T$ , we obtain  $\lambda_p \sim 10^{-5}$   $\text{cm}^2 \text{s/g}$ .
- [14] F. Brochard and J.-F. Lennon, *J. Phys. (Paris)* **11**, 1035 (1975).
- [15] A typical channel opens for about  $\tau \sim 1$  ms (see, e.g., Ref. [3], pp. 525–531) during which about  $10^3 - 10^4$  ions pass through [5].